THE ASTROPHYSICAL JOURNAL, 438:341–349, 1995 January 1

OPTICAL SPECTROSCOPY OF CARBON-RICH PROTO–PLANETARY NEBULAE

BRUCE J. HRIVNAK[1]
Department of Physics and Astronomy, Valparaiso University, Valparaiso, IN 46383; e-mail: bhrivnak@exodus.valpo.edu
and Dominion Astrophysical Observatory, Herzberg Institute of Astrophysics, 5071 W. Saanich Rd.,
Victoria, BC Canada V8X 4M6
Received 1994 February 28; accepted 1994 July 8

ABSTRACT

In this paper, we present a medium-resolution (3 Å) spectroscopic study of six proto–planetary nebulae, post–asymptotic giant branch (AGB) objects with large infrared excesses. All six are found to display the spectra of G supergiants. However, they also show molecular carbon features, C_2 and in most cases C_3, and strong absorption lines due to *s*-process elements. Other evidences of a carbon-rich nature are found in published molecular-line millimeter emissions (CO and HCN) and 3.3 μm features attributed to polycyclic aromatic hydrocarbons. These properties are all in accord with what one would expect in a post–AGB star in which carbon-rich materials formed in thermal pulses is dredged up to the surface of a mass-losing object. A correlation is found between the presence of molecular C_2 absorption and the presence of the unidentified 21 μm emission feature. This strengthens the suggestion that carbon is a major component of the molecule producing this unidentified feature. Four additional proto–planetary nebulae which share some of these properties are also discussed.

Subject headings: circumstellar matter — stars: abundances — supergiants — stars: evolution — stars: AGB and post–AGB

1. INTRODUCTION

The study of proto–planetary nebulae (PPNs) is one of the areas in stellar astrophysics which has benefited greatly from the successful *Infrared Astronomical Satellite* (*IRAS*) mission. PPNs are objects in transition between the asymptotic giant branch (AGB) and planetary nebula (PN) stages of evolution. Observations show that objects on the AGB are losing mass at an increasing rate as they evolve toward the tip of the AGB. Theoretical models indicate that objects in this stage possess a core of oxygen and carbon surrounded by helium and hydrogen-burning shells. Thermal pulses may develop in the helium-burning shell which produce neutron-rich, *s*-process isotopes. These *s*-process elements and recently produced carbon are then dredged up to the surface (Iben & Renzini 1983). Thermal pulses may also contribute to the mass-loss process. When the mass in the envelope has dropped to 10^{-3} $M_\odot$, the major stage of mass loss has ended (Schönberner 1983). The now detached gas shell expands away from the object, with dust grains forming at a distance where the temperature is below the condensation temperature of the grains. The central star, meanwhile, evolves at approximately constant luminosity toward higher temperatures (horizontally to the left of the H-R diagram). When the temperature of the central star reaches ~30,000 K, it is sufficient to begin to ionize the circumstellar gas shell and the object will appear as a PN. The timescale of the transition from the detaching of the shell to the PN stage is a few thousand years for typical core masses of 0.55–0.65 $M_\odot$ (Schönberner 1983, 1990).

Observationally, one would expect PPNs to possess expanding circumstellar envelopes of gas, emission from dust, and central stars of high luminosity and intermediate spectral types. This is exactly what has been observed. Infrared emission indicative of a dust temperature of 150–300 K, as derived from the *IRAS* data, has been used to guide the choice of PPN candidates (Volk & Kwok 1989). CO or OH emission has been observed from PPN candidates, with typical expansion velocity of ~15 km s^{-1} (Likkel et al. 1991; Likkel 1989). Some of the PPN candidates possess bright optical counterparts (V = 7–11 mag), with optical spectra indicating the central stars as A–G supergiants (Parthasarathy & Pottasch 1986; Hrivnak, Kwok, & Volk 1989; van der Veen, Habing, & Geballe 1989; Trams et al. 1991). Model fits to the optical and infrared fluxes, combined with gas expansion velocities, yield ages of about a thousand years since the shells detached (Hrivnak et al. 1989). Kwok (1993) has recently reviewed the properties of PPNs and listed 28 good candidates, including the six in this study.

In this paper, we examine in detail the optical spectra of six PPNs—IRAS 04296+3429, 05113+1347, 20000+3239, 22223+4327, 22272+5435, and 23304+6147. All six were initially selected as PPN candidates based upon their *IRAS* colors. By the use of ground-based observations at 10 μm, we accurately located the positions of the objects and found all six to have bright (V = 9–14 mag) optical counterparts. Finding charts of 04296+3429 and 23304+6147 have been published by Hrivnak & Kwok (1991a); charts for the others will be published elsewhere (Hrivnak et al. 1994). Here we describe the spectra and report the discovery of molecular carbon absorption features in the visible spectra of all six. The origin of these features and their correlation with other unusual spectral features are discussed. One of these objects, 22272+5435 (HDE 235858), has previously been discussed separately (Hrivnak & Kwok 1991b); for the other five, this is the first discussion of their optical spectra.

2. OBSERVATIONS

Observations of four of our primary sources were made over several wavelength ranges on various nights in 1989 and 1990

[1] Visiting Astronomer, Kitt Peak National Observatory, National Optical Astronomy Observatories, operated by the Association of Universities for Research in Astronomy, Inc., under contract with the National Science Foundation.

TABLE 1

Observational Log

Object	Wavelength (Å)	R(Å)	Date	Observatory	Figure
Program Objects					
04296+3429......	3872–4870	2.6	1991 Sep 23	KPNO	1, 2
05113+1347......	3872–4870	2.6	1991 Sep 23	KPNO	1, 2
20000+3239......	3872–4870	2.6	1991 Sep 23	KPNO	1, 2
	3908–4880	4.8	1990 Jul 17	DAO	
	4562–5210	4.5	1990 Jul 18	DAO	3
	5808–6785	2.9	1989 Jul 25	DAO	4
22223+4327......	3900–4520	3.4	1989 Nov 22	DAO	1, 2
	3908–4880	4.8	1990 Jul 17	DAO	
	4562–5210	2.3	1990 Jul 18	DAO	3
22272+5435......	3880–4770	3.0	1989 Jul 24	DAO	1, 2
	3990–4520	3.4	1989 Nov 22	DAO	
	4562–5210	2.3	1990 Jul 18	DAO	3
	5808–6785	2.9	1989 Jul 25	DAO	4
23304+6147......	3872–4870	2.6	1991 Sep 23	KPNO	1, 2
	5808–6785	2.9	1989 Jul 25	DAO	4
Related Objects					
AFGL 2688	3874–4520	2.8	1990 Jul 20	DAO	2
	5808–6785	3.4	1989 Jul 25	DAO	4
07134+1005......	4576–5226	4.7	1990 Jan 18	DAO	5

at the Dominion Astrophysical Observatory (DAO). The 1.8 m telescope was used with the facility Cassegrain spectrograph and either the Ford 512 × 512 or RCA 620 × 1024 CCD chips. The resolution varied between 2.3 and 4.8 Å, depending upon the slit width used. Spectra of an Fe-Ar arc were obtained before and after each stellar spectrum and used for the wavelength calibration.

Observations of four of the objects were made at the Kitt Peak National Observatory (KPNO) on 1991 September 23, using the 2.1 m telescope. The Gold Camera Cassegrain CCD Spectrometer was used, with a TI 800 × 800 chip and the "26 new" grating. This combination produced a spectrum of slightly less than 1000 Å width and a resolution of 2.6 Å. Spectra of a He-Ne-Ar emission source were obtained before and after each of the stellar spectrum and used for wavelength calibration.

In Table 1 we have listed a log of these observations, including wavelength range, spectral resolution, UT date of observation, and observatory. Most of these spectra are displayed in subsequent figures in this paper. In addition, spectra of several standard stars were observed for comparison.

The spectra were reduced using IRAF[2] at the DAO. They were bias-substracted, flat-field–corrected with respect to a lamp, sky-subtracted, and wavelength-calibrated to produce the final one-dimensional spectra. The spectra were not flux-calibrated and included the instrumental responses.

3. DESCRIPTION OF THE SPECTRA

3.1. *Classification*

The spectra were classified using the ratios of features as discussed in Keenan & McNeil (1976) and Yamashita, Nariai, & Norimoto (1978), and comparison with spectra of standards which we obtained with the same instrumentation. The program star spectra are shown in Figure 1. The spectra appear to span the G spectral types and show features indicative of high luminosity. Also the Ba II λ4554 feature is very strong, and molecular C_2 at λ4737 is obvious. To help classify the spectra, we had at our disposal spectra of the very luminous supergiants HR 8752 (G5 0–Ia) and HD 6474 (G4 0–Ia), and spectra of the supergiants HR 7847 (F5 Iab), HR 7796 (F8 Ib), HR 8313 (G5 Ib), HR 8321 (K0 Ib), and HR 7475 (K4 Ib). [The spectral types of all but the last of these standards are taken from Keenan & McNeil (1976) and Yamashita et al. (1978).] These spectra were obtained at the DAO using the same instrumental arrangements.

The luminosity classification is complicated by the evidence for enhancement of *s*-process elements such as Ba, Sr, and Y, since Sr II and Y II are among the primary features used in luminosity classification. In addition to the strong Ba II feature at λ4554, Sr II λ4077, Y II λ3983, and Y II λ4375 are also strong (as well as some other lines of these elements which we will discuss later). We show on an expanded scale the spectra between 3900 and 4280 Å in Figure 2, along with several standards and the well-known PPN AFGL 2688 (Egg nebula), which we will discuss later. The ratio Sr II λ4077/Fe $\lambda\lambda$4063+4071 would indicate that 04296+3429, 23304+6147, and 22223+4327 are all at least of luminosity class Ib, and that 22272+5435, 20000+3239, and 05113+1347 are Ia or 0. The Sr II, Fe λ4216 feature could not be used because of the appearance of the CN 4216 band head, which is visible in all of these spectra, and is strong in 22272+5435, 05113+1347, and 20000+3239. The $\lambda\lambda$4172+4178 blend/Hδ ratio is a sensitive criterion at high luminosities, with the λ4178 feature as compared with λ4172 increasing more rapidly with increasing luminosity and increasing temperature. In all six of our program stars λ4178 is stronger than λ4172, an effect not seen in any of our supergiant standards; perhaps this is due to the contribution of Y II λ4178. The ratio λ4172/Hδ indicates Ib for

[2] Image Reduction and Analysis Facility (IRAF) is distributed by the National Optical Astronomy Observatories which is operated by the Association of Universities for Research in Astronomy, Inc., under contract to the National Science Foundation.

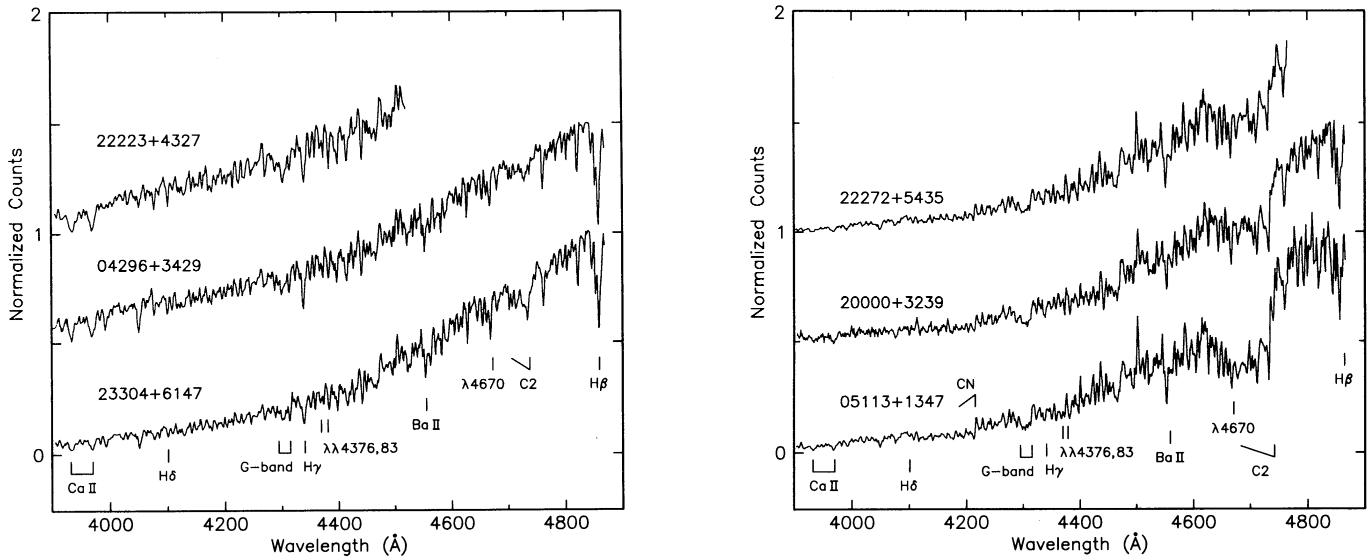

FIG. 1a FIG. 1b

FIG. 1.—Spectra of the six program objects in the wavelength interval 3900–4870 Å, with a resolution of about 3 Å. (The spectra are normalized and shifted arbitrarily in counts for display purposes; they have not been corrected for the lower detector response at the shorter wavelengths.) Several of the prominent features are marked. The spectrum of 20000+3239 is extremely noisy below 4100 Å.

04296+3429, 23304+6147, and 22223+4327, and 0–Ia for the other three, but caution must be exercised due to the effects of the strong CN band at λ4216. Keenan & McNeil (1976) make the remark that in the stars which they show with barium enhancement, the λ4376/λ4383 ratio behaves almost normally, even though λ4376 is a blend involving Y II. The Y II, Fe 4376 feature is very strong in all of our program objects, in some cases comparable to the strength of the Fe λ4383 feature. The λ4376/λ4383 ratio in these program objects is at least as strong as in the spectra of the two extremely luminous supergiants standards observed, indicating an extremely high luminosity and/or an extremely high yttrium abundance. The Fe λ4442/λ4435 blend and the Fe, Ti II λ4409/Fe λ4404 ratios suggest Ia for all six, and the G band indicates Ia or Iab, particularly the strength of the λ4314 line. Thus we conclude all six to be of luminosity class Ia, and note the strong lines of the *s*-process elements.

To classify the spectral type we used the following features: Fe, CH λ4325/Hγ and Fe λ4143/Hδ were the primary feature ratios, with λ4046/Hδ rendered less useful because of blending with the strong feature at λ4050 which we will discuss later. The spectral types determined range from G0 to G8 and are

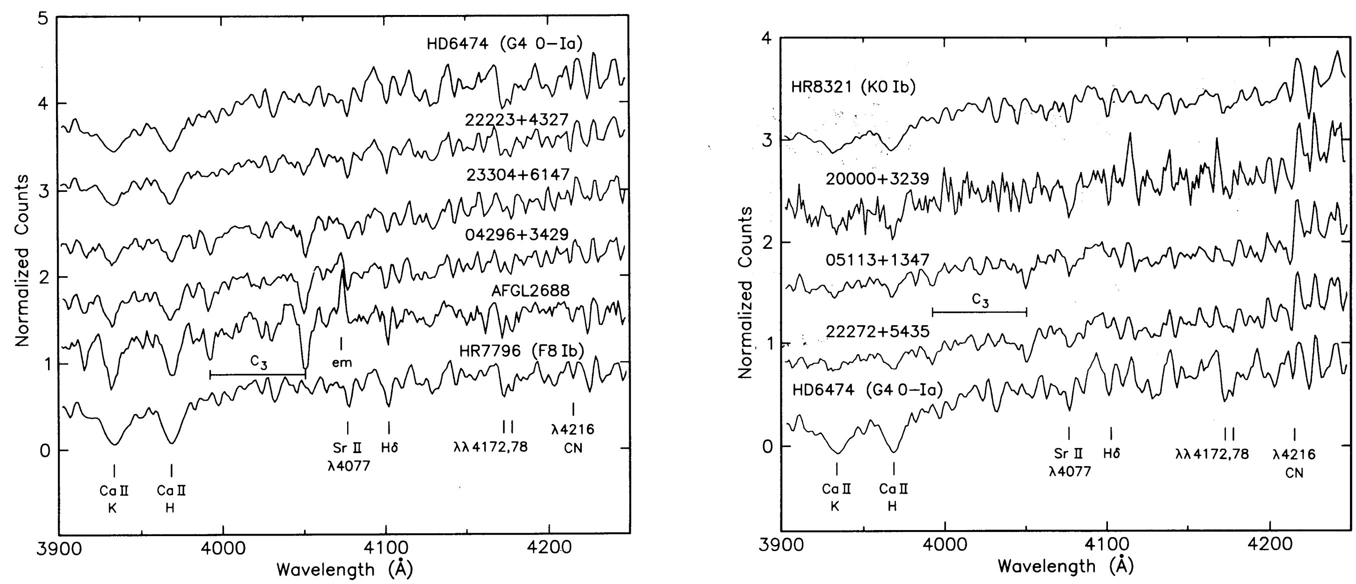

FIG. 2a FIG. 2b

FIG. 2.—Spectra of the six program stars expanded from Fig. 1 to show details of the spectral features. The spectrum of 20000+3239 is extremely noisy below 4100 Å. Several standard stars observed at a similar resolution are also shown for comparison. The spectrum of 22223+4327 is at somewhat lower resolution than are the others; see Table 1 for details.

listed in Table 2. Hδ appears weak in 05113+1347 and 22272+5435. Note that in 05113+1347 and 20000+3239, the feature at λ4337 (Fe + Cr + Ti II) appears as a shortward blend with λ4339 (Hγ + Cr). In all six, Ca I λ4226 appears weak in comparison to the Ib and 0–Ia standards, and there is a suggestion that perhaps it is filled in by emission. The λλ4172, 4178 pair of lines is known to show a temperature effect, with λ4178 decreasing with decreasing temperature. As mentioned above, in all six of our primary program objects λ4178 is stronger that λ4172, which suggests a spectral type earlier than early-G or/and a very high luminosity. However, this is probably strongly affected by Y II at λ4178. If chemical peculiarities are suspected, Keenan & McNeil (1976) suggest using the Cr λ4254/Fe λλ4250, 4260 ratio. When this ratio was compared for these six objects, the ratio of 22223+4327 was similar to HD 6474 (G4 0–Ia), while in 04296+3429 and 23304+6147 λ4254 is stronger than the other two lines, suggesting a spectral type later than K0, and in the three other (cooler) objects λ4250 was very weak or absent and λ4260 was weak compared with λ4254, suggesting an even later spectral type. However, Sc II 4247 was even stronger than λ4254 in all six program objects, an effect seen in early to mid-G very luminous supergiants, so there must be some other effect which complicates these ratios. Note that in the spectra of 05113+1347, 20000+3239, and 22272+5435, there appears a feature at 4504 Å which initially might appear to be an emission feature (see Fig. 1*b*). In fact, we judged this to instead indicate the level of the continuum in the presence of many overlapping absorption lines and bands. A similar effect is noticeable in the published photographic spectrum of RW Cep (K0 0–Ia; Yamashita et al. 1978).

Spectra of three of our program objects were obtained in the region λλ4560–5210, which includes Hβ and several C_2 bands. These are shown in Figure 3 and have a spectral resolution (determined from the width of the calibration arc lines) of 2.3 Å, except for 20000+3239, which is a factor of 2 lower. Jaschek & Jaschek (1987) suggest λ4921/Hβ to be a good ratio for classification in the region near λ5000. Comparison of spectra of 20000+3239, 22223+4327, and 22272+5435 with our observed spectra standards suggests somewhat later spectral types than those derived in the blue. However, any weakening or infilling by emission in the Hβ line will greatly affect this classification in the same way. The prominent C_2 band at λ5165 will be discussed below.

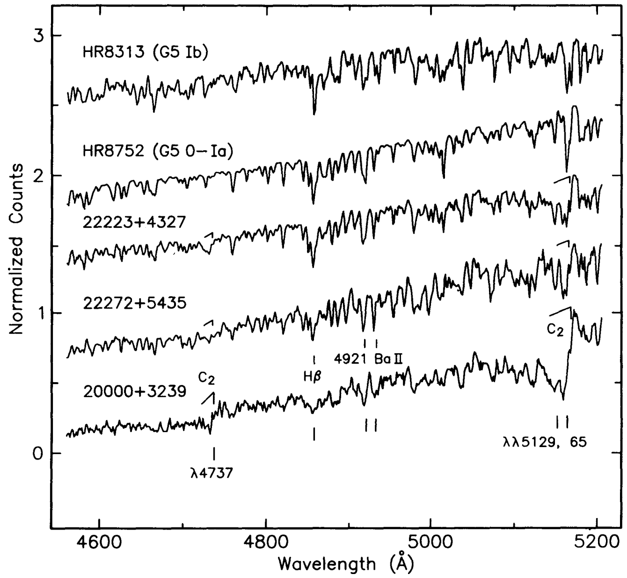

FIG. 3.—Spectra of three program objects and two standard stars in the wavelength interval 4560–5210 Å. These show Hα and Swan C_2 bands. Note that the resolution of 20000+3239 is a factor of 2 lower.

Observations of three of the program objects were also made in the spectral region including the Na D doublet and Hα from ~5800 to 6800 Å, with a resolution of about 3 Å. (Note that

TABLE 2

OBSERVATIONAL SUMMARY: PROGRAM AND RELATED STARS

Object	Other Names	*b*	*V*	*B*−*V*	*E*(*B*−*V*)	Spectral Type	Carbon Features
			Program Objects				
04296+3429......	...	−9	14.2[a]	2.0	1.3	G0 Ia pec	C_2, C_3
05113+1347......	...	−14	12.4[b]	2.1	1.0	G8 Ia pec	C_2, C_3
20000+3239......	...	+1	13.3[b]	2.8	1.7	G8 Ia pec	C_2
22223+4327......	DO 41288	−12	9.7[b]	0.9	0.2	G0 Ia pec	C_2, C_3
22272+5435......	HDE 235858; SAO 34504	−3	8.7–9.5[c]	1.9	0.9	G5 Ia pec	C_2, C_3
23304+6147......	...	+1	13.1[a]	2.3	1.5	G2 Ia pec	C_2, C_3
			Related Objects				
07134+1005......	HD 56126; SAO 96709	+10	8.2[d]	0.9	0.5	F5 I	C_2
AFGL 2688	Egg nebula	−6	12.2[e]	1.1	0.7	F5 Iae	C_2, C_3[f]
05341+0852......	...	−12	12.8[g]	...	...	F:	
08005−2356......	...	+4	11.5[h]	1.4	1.0	F5 Iae	C_2, C_3[h]

Sources for magnitude data, and for spectral information if not this paper.
[a] Hrivnak & Kwok 1991a.
[b] Hrivnak et al. 1994.
[c] Hrivnak & Kwok 1991b.
[d] Hrivnak, Kwok, & Volk 1989.
[e] Ney et al. 1975.
[f] Crampton, Cowley, & Humphreys 1975; Cohen & Kuhi 1977.
[g] Guide Star Catalog (Jenkner et al. 1990).
[h] Slijhuis, Hu, & de Jong 1991.

the signal-to-noise ratio is lower in 20000+3239 and 23304+6147 than in 22272+5435.) These were made to particularly investigate evidence for Hα emission and to look for any other peculiarities in the spectra. These are displayed in Figure 4*a*, where we also show for comparison the spectra of two luminosity class Ib supergiants. Several obvious differences can be seen. The shape of the continuum is much steeper for the PPNs; this is due to the large amounts of reddening of these objects, which are listed in Table 2. Hα absorption is considerably weaker in the PPNs, an effect which was suggested to be present at Hβ. The Ba II λ6497 line is strong, consistent with the strong Ba II line observed in the blue region.

We have summarized the spectral classification of these six objects in Table 2, along with some photometric data and their galactic latitudes *b*. They range from G0 to G8; it should be remembered that all six are chemically peculiar. The reddening is determined by comparing the observed colors with the intrinsic colors of supergiants, using a summary table by Gray (1989).

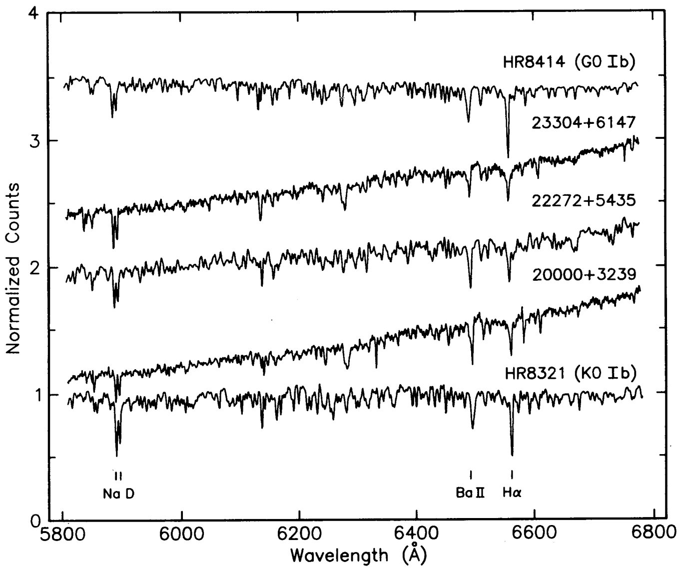

FIG. 4*a*

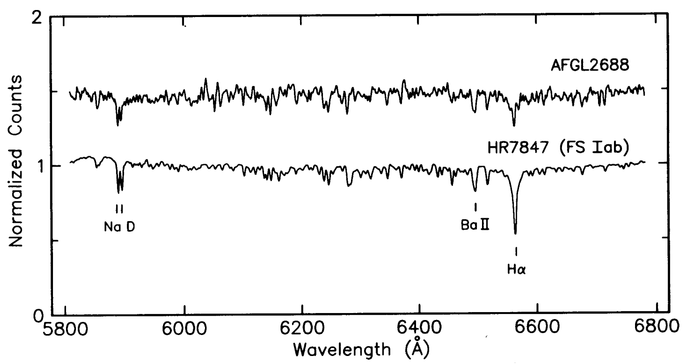

FIG. 4*b*

FIG. 4.—(*a*) Spectra of three program objects and three standards in the wavelength interval 5800–6800 Å, which includes the Na D doublet and Hα. Note in the PPNs the weakness of the Hα feature and also the slope in the continuum due to reddening. (*b*) Spectra of AFGL 2668 and the spectral standard HR 7847 (F5 Iab). Note the apparent infilling of the Hα feature by emission. (The resolution is slightly lower than in Fig. 4*a*).

3.2. C_2 *and* C_3

The Swan bands of molecular C_2 are seen in the spectra of all six of these PPN candidates at λ4737 and λ4715. In Figure 1 strong features are seen in the cooler three, but the absorption band is also visible in 23304+6147 and 04296+3429. While the displayed spectrum of 22223+4327 does not extend to this wavelength, a lower resolution spectrum extending from 3900 to 4880 Å clearly shows the feature. For several of these objects, we also obtained spectra which show the stronger band head at λ5165. These are shown in Figure 3 for 22223+4327, 22272+5435, and 20000+3239; note that the resolution is lower for 20000+3239. The C_2 feature is distinct in wavelength from the Mg *b* feature seen in HR 8752 and HR 8313, which are shown for comparison. The C_2 features at λ5165 and λ5129 and also at λ4737 appear comparable or stronger in 22223+4327 than in 22272+5435. Thus while the C_2 features follow a general trend in these spectra of increasing in strength with decreasing temperature, this is not strictly true; they are stronger in 05113+1347 (G8) than in 20000+3239 (G8), and comparable in strength in 22223+4327 (G0) to 22272+5435 (G5). The $^{12}C^{13}C$ band head at λ4744 appears to be present in 05113+1347 and possibly 22272+5435.

Molecular C_3 is also seen in the spectra of five of these PPNs at λ4050, λ3991, and perhaps λ3915. It appears to be weaker, however, in 22223+4327 and the feature at λ3991 may be absent. C_3 seems to be absent from 20000+3239, although this spectrum is very weak and noisy shortward of λ4077. This spectral region is shown in Figure 2. The presence of C_3 in a stellar spectrum is extremely rare, having been reported previously only for the PPNs AFGL 2688 (Crampton, Cowley, & Humphreys 1975) and 22272+5435 (Hrivnak & Kwok 1991b), for the obscured carbon star IRC +10216 (Hinkle, Keady, & Bernath 1988), and for late N-type carbon stars (McKeller 1948; Swings, McKeller, & Rao 1953).

3.3. *S-Process Elements*

Absorption lines due to the *s*-process elements Ba, Sr, and Y are quite strong in these program objects. The Ba II line at λ4554 is quite strong in all six, especially in the cooler ones. The Ba II lines at 4934 Å and 6497 Å are also strong. The strong line at λ3983 is due to Y II, and the strong features at λ4178 (see Fig. 2 and the above discussion) and λ4375 are due partly to Y II. Sr II produces the strong line at λ4077, which is usually used as a luminosity indicator. These lines all have a strong luminosity effect which complicates their interpretation. An abundance study using higher resolution spectra and spectrum synthesis modeling would be helpful to quantify the abundance of the *s*-process elements in these objects.

3.4. *Comments on Individual Spectra*

04296+3429.—The spectrum is classified as G0 or perhaps F8. The Y II λ3983 line is very strong. A feature appears to be in emission at λ4071, close to the wavelength of an emission feature in AFGL 2688 (see Fig. 2*a*) which has been attributed to [S II] blend of λ4069 and λ4076 (Crampton et al. 1975).

05113+1347.—The spectral type appears to be G8, or possibly as late as K0. The C_2 and C_3 absorption features are quite strong.

20000+3239.—The spectral type is G8 or possibly K0. Hδ appears weak. In this object, Y II, Fe λ4376 is stronger than Fe λ4383, which is unusual. The C_3 features at λ4050 and λ3991 are not seen, but this may be due to the weakness of the spectrum at $\lambda < 4077$ Å.

22223+4327.—The spectrum appears to be G0–F8. The Y II λ3983 is not as strong as in the other PPNs. The C_3 feature at λ4050 is present, but weak, and the presence of the feature at λ3991 is questionable.

22272+5435.—The spectral type is classified as G5. Hδ appears weak. Spectra of this object have previously been displayed and discussed by Hrivnak & Kwok (1991b), who called attention to the molecular carbon features and classified the spectrum as Gp Ia.

23304+6147.—The spectrum appears as G2. The line at 4085 Å is relatively stronger than in the other PPNs or supergiants.

3.5. *Observations of Related Objects*

AFGL 2688.—AFGL 2688 (the Egg nebula) appears optically as two small lobes separated by ~8″. They are generally regarded as reflection nebula from an object in the PPN stage.

The spectrum of this object was discussed previously by Crampton et al. (1975), who classified the spectrum as F5 Ia in the region 4100–5000 Å. In addition, they identified absorption features in the region 3870–4050 Å which they attributed to C_3 and a few emission features attributed to C_2 and [S II]. Cohen & Kuhi (1977) obtained polarization measurements with a spectrum scanner. While the total flux showed C_2 in emission, the polarized light clearly showed C_2 in absorption at $\lambda\lambda$5165, 5129, 5635, 5585, 4737. This suggests that the light from the hidden, central star, containing C_2 in absorption, is scattered and polarized in the lobes, and that C_2 in the lobes is producing emission. They also cited the presence of SiC_2 absorption. Cohen & Kuhi (1977) classified the underlying star as F2 I.

Both Crampton et al. (1975) and Humphreys, Warner, & Gallagher (1976) noted the weak Hα absorption feature, which they suggested is filled in by emission. Humphreys et al. cited the presence of Na I D emission in their echelle spectrum of AFGL 2688.

We have obtained a spectrum of the brighter lobe of AFGL 2688 in the spectral region from 3874 to 4520 Å. This is shown in Figure 2*a*. A spectral classification based upon the ratio Fe $\lambda\lambda$4144/4173 indicates F2, while Ca $\lambda\lambda$4227/Hδ indicates F8. Thus an F5 classification is a compromise between these two. However, if there is emission filling in some of the hydrogen lines, then the earlier spectral type is preferable. The luminosity is classified as Ia based upon comparison with standards and in particular the ratio $\lambda\lambda$4313/4325. The Sr λ4077 line, which is a typical luminosity indicator, is weak and presumably affected by the nearby emission feature. This emission feature is at 4073 Å, and Crampton et al. (1975) attributed it to the blend [S II] $\lambda\lambda$4069, 4076. In addition, absorption features attributed to C_3 are seen at $\lambda\lambda$4051, 3992, and possibly $\lambda\lambda$3915, 3879. The spectrum from 5800 to 6600 Å is displayed in Figure 4*b*. The Hα line is present in absorption, but weaker than expected for an early- to mid-F star, and the line profile shows evidence for Hα emission superposed on the absorption feature. The Na I D absorption lines are strong, the Ba II λ6497 is seen in absorption.

07134+1005.—IRAS 07134+1005 (HD 56126, SAO 96709) has been identified as a PPN by Hrivnak et al. (1989). They show a spectrum from 3920 to 4560 Å which they classify as an F0–5 supergiant; Nassau, Stephenson, & MacConnell (1965) have classified the spectrum as F5 I. In a recent high-resolution spectroscopic study to determine its chemical composition, Parthasarathy, Garcia Lario, & Pottasch (1992) found 07134+1005 to be metal-poor, [Fe/H] ≤ -1.0, with carbon, oxygen, and sulfur possessing nearly solar abundances and nitrogen slightly overabundant when compared with the Sun. We were motivated to compare 07134+1005 with the program stars because, in common with them, it possesses infrared emission features at 21 μm (Kwok, Volk, & Hrivnak 1989) and 3.3 μm (Kwok, Hrivnak, & Geballe 1990), and also a carbon-rich circumstellar envelope (Omont et al. 1993).

In Figure 5 we show a spectrum of 07134+1005 covering the region from 4600 to 5200 Å at a reduction of 4.7 Å. A spectrum of HR 8752 (G5 0–Ia) obtained with the same instrumental set up and resolution is shown for comparison. We see in 07134+1005 the strong line of Hβ and lines at $\lambda\lambda$4923, 4934 (Ba II), λ5019. In addition, C_2 features appear to be present at λ5165 and λ4737. The C_2 feature at λ4737 appears distinctly in 07134+1005. The strong Mg *b* feature at λ5167 interferes with C_2 λ5165, but C_2 seems to be present. The spectrum of 22223+4327, displayed previously in Figure 3 but now smoothed to lower the resolution ($R = 5.6$ Å), is also shown in Figure 5 for comparison.

4. CORRELATIONS BETWEEN MOLECULAR CARBON FEATURES AND INFRARED EMISSION FEATURES

While these objects are unusual in that they each show molecular carbon in their optical spectra, they also have several other spectral properties in common. These are summarized in Table 3. The most outstanding of these is the presence of an unidentified emission feature at 21 μm. This feature was first identified in the *IRAS* Low-Resolution Spectrometer (LRS) spectra of three of these six program objects. 04296+3429, 22272+5435, 23304+6147, and the related object 07134+1005 (Kwok et al. 1989). It was later identified in a fifth object, IRAS 22574+6609, a cool *IRAS* source with only a very faint ($V = 24$) optical counterpart (Hrivnak & Kwok 1991a). The *IRAS* LRS spectra of 05113+1347 and 20000+3239 were suggestive of a weak 21 μm feature, and this has recently been confirmed in both of these objects and also in 22223+4327 and IRAS 05341+0852 by ground-based 10 and 20 μm spectroscopy (Kwok et al. 1993). Thus we see that all six of our program objects possess the 21 μm emission feature. To

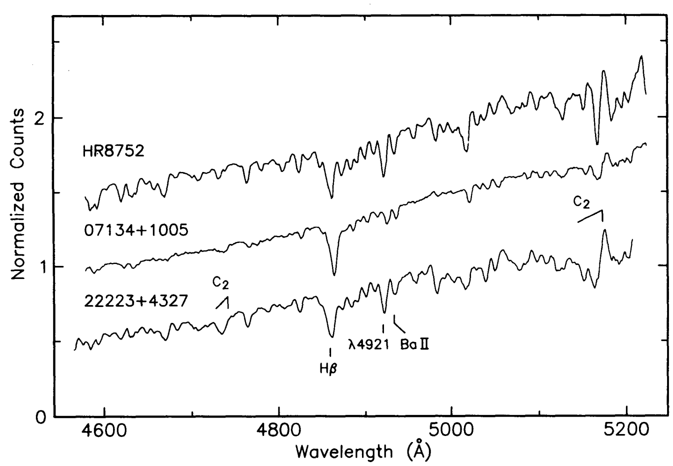

FIG. 5.—The spectrum of 07134+1005 in the region 4600–5200 Å, with HR 8752 (G5 0–Ia) and 22223+4327 for comparison. The resolution is 4.7 Å for 07134+1005 and HR 8752, 5.6 Å for 22223+4327.

TABLE 3

SUMMARY OF SPECTRAL FEATURES, EMPHASIZING CORRELATION WITH CARBON

Object	Spectral type	C_2	C_3	3.3 μm	3.4 μm	Molecular Line[a]	21 μm
			Program Objects				
04296+3429......	G0 Ia	Y	Y	Y	≈Y	CO, HCN	Y
05113+1347......	G8 Ia	Y	Y	Y:	N	...	Y
20000+3239......	G8 Ia	Y	N	...	...	CO, HCN	Y
22223+4327......	G0 Ia	Y	Y:	...	...	CO, HCN	Y
22272+5435......	G5 Ia	Y	Y	Y	≈Y	CO, HCN, CS	Y
23304+6147......	G2 Ia	Y	Y	...	...	CO, HCN	Y
			Related Objects				
AFGL 2688	F5 Iae	Y	Y	Y	Y	CO, HCN, HC_xN[b]	N
07134+1005......	F5 I	Y:	N	T	N	CO, HCN	Y
05341+0852......	F:	...	...	Y	≈Y	...	Y:
08005−2356......	F5 Iae	Y	Y:	...	...	OH, (CO:ND)[c]	N

[a] Omont et al. 1993, unless noted otherwise.
[b] Olofsson 1987.
[c] Likkel 1989.

date, the 21 μm feature has been observed only in PPNs. The 21 μm feature also seems to be accompanied by an emission plateau from 11 to 15 μm.

Another similarity among the program objects is seen in their 3 μm spectra. Three of them have been observed in this spectral region. Two of them, 04296+3429 and 22272+5435, possess a strong 3.3 μm emission feature and the third, 05113+1347, may have a weak feature (Hrivnak, Kwok, & Geballe 1994). This 3.3 μm feature is commonly attributed to polycyclic aromatic hydrocarbons (PAHs), and these are the coolest objects known to display the PAH features. What is particularly unusual is that the former two of these possess a 3.4 μm emission feature comparable in strength to the 3.3 μm feature (Geballe et al. 1992). This is quite unusual, having been observed previously only in the PPN candidate 05341+0852 (mentioned above) and in Nova Cen 1986 (Geballe & van der Veen 1990). The other three of our program objects have not been observed spectroscopically at this wavelength, and thus we do not know if they all possess the 3.3 μm feature and how common is the strong 3.4 μm feature among these objects. Among the related objects, AFGL 2688 also has a 3.3 μm and a relatively strong 3.4 μm emission feature (Geballe et al. 1992), and 0713+1005 has the 3.3 μm but not strong 3.4 μm feature (Kwok et al. 1990).

IRAS 22272+5435 has also been found to possess a strong, broad emission feature at around 30 μm in spectra observed from the Kuiper Airborne Observatory (Omont 1993). A 30 μm excess has been found previously in several carbon-rich AGB objects and PNs, such as NGC 7027, but only the PN IC 418 has as strong a feature as does 22272+5435 (Cox 1993). IRAS 23304+6147 is found to have a 30 μm excess, while the related object 07134+1005, which also has the 21 μm emission feature, does not (Omont 1993). While the presence of the strong 30 μm feature, in addition to the 21 μm, 3.4 μm, C_2, and C_3 features, in 22272+5435 is interesting, the lack of observations of most of the program stars in the 20–50 μm range precludes one from drawing conclusions about a correlation of the 30 μm feature with the molecular carbon features observed in the optical spectrum.

Molecular-line observations at millimeter wavelengths have been made of all of our program objects except 05113+1347. All five observed were found to be strong emitters at CO (2–1) and HCN (1–0), and the strong HCN is regarded as strong evidence of the carbon-rich chemistry of their circumstellar shells (Omont et al. 1993). CO and HCN emissions have also been detected from 07134+1005, although the HCN/CO ratio for this object is smaller than for the other 21 μm sources (Omont et al. 1993), and the $^{13}CO/^{12}CO$ ratio is unusually weak (Bujarrabal, Alcolea, & Planesas 1992). AFGL 2688 (Egg nebula) is a well-known source of emission from carbon-chain molecules (Olofsson 1987). OH has been searched for in four of the sources—04296+3429, 22223+4327, 22272+5435, 23304+6147—but not detected. OH has also been searched for and not detected in the related objects 05341+0852, 07134+1005, and AFGL 2688 (see Omont et al. 1993, Tables A1 and A2, and references therein; 05341+0852: Lewis, Eder, & Terzian 1990).

In Table 3 we have summarized the spectral features of these objects as they seem to be related to their carbon-rich nature. We have also included similar information on several related objects. Note that little is known in the visible about the related object 05341+0852; however, we have recently obtained photometry and spectroscopy of it which we will reduce and discuss elsewhere.

5. DISCUSSION

We have found all six of our program objects to have the spectra of G supergiants. All six display C_2 and most of them C_3 absorption features, indicating that they are carbon-rich. The millimeter molecular-line observations support this interpretation. This is consistent with what one would expect as a result of the dredge-up of carbon-rich material formed in thermal pulses (third dredge-up) to the outer layers of a star whose envelope has been depleted by significant mass loss (Lattanzio 1989). An enhancement of *s*-process elements is also seen, again consistent with this interpretation. While the appearance of these features is not surprising in the spectra of objects which are thought to be in the post–AGB phase, it is nevertheless strong observational evidence to support this claim.

Note that while we have not done a chemical abundance study, these program objects clearly do not possess the extremely large underabundance in metals seen on some post–

AGB objects, such as HR 4049 (Lambert, Hinkle, & Luck 1988; Waelkens et al. 1991) and HD 52961 (Waelkens et al. 1991). Other post–AGB objects, such as BD +39°4926, HD 46703, and HR 4912, have also been found to have low metal abundances (see review by Bond 1991). All of these objects except HD 52961 are found at high galactic latitudes ($b \geq 20°$), in most cases are low in *s*-process elements (Luck & Bond 1989), and are interpreted as low-mass post–AGB stars. The infrared excesses of these objects, while they are significant in some cases (while other ones have not been detected with *IRAS*), are not nearly as large as in the sample of program objects discussed in this paper. In contrast, the program objects discussed in this paper appeared to have normal metal abundances, are high in *s*-process elements, are carbon-rich, and are at lower galactic latitudes (see Table 2). We suggest that the differences between these two samples of evolved stars arise because our carbon-rich program objects may be younger and have had progenitors of higher (intermediate) mass.

The correlation of a carbon-rich chemistry, as evidenced by the C_2, C_3 and HCN, with the 21 μm emission feature adds increased support to the suggestion of Kwok et al. (1989) that carbon is a major constituent of the molecule producing this feature. It appears that the carbon-rich composition and the particular environment found in these transition objects permits the molecule to be formed and excited without destroying it. This 21 μm feature is not seen in the preceding evolutionary phase, where the AGB object is continuing to lose mass, nor in the succeeding PN state, where the central star is much hotter and the circumstellar envelope is ionized. This sample seems to indicate that it happens when the central star is between a late-G and mid-F spectral type.

We have previously noted the presence of the 3.3 μm emission feature in all of our objects which have been observed in this wavelength region. Spectroscopic observations of 22272+5435 between 5.0 and 13.5 μm and of 07134+1005 between 5.0 and 8.3 μm are reported by Buss et al. (1990). They show a number of infrared emission bands similar to those seen in H II regions and PNs. IRAS 22272+5435 displays the 6.2 and 6.9 μm features. However, rather than the usual 7.7 μm emission feature, they find a feature at 8 μm. Similarly, rather than an 11.3 μm emission feature, they find a broad feature at 12 μm. We mentioned earlier the unusually strong 3.4 μm feature. Thus these transition objects seem to possess features similar to, but yet somewhat different from, the well-known infrared emission features seen in PNs. Recent observations of 22272+3435 with a ground-based spectrometer at a higher resolution than the *IRAS* LRS spectra seem to show structure in the 21 μm feature and in the 11–13 μm plateau (Barlow 1993).

The location of the observed molecular C_2 and C_3 is presumably in an extended atmosphere of these objects, and thus represents the chemistry of the star. The infrared emission features and the molecular-line emission originate in the circumstellar envelope of dust and gas, and represent the chemistry of the star during its AGB mass-loss phase. In the case of the six program objects and the related objects 07134+1005 and AFGL 2688, the chemistry is the same in both regions. An interesting object with a large infrared excess, and which may be related to these program objects, is IRAS 08005−2356. It has been studied by Slijkhuis, Hu, & de Jong (1991), who identified it with a bright ($V = 11.5$) F5 Ia star. The spectrum shows emission lines with P Cygni profiles, suggesting ongoing mass loss. The spectra which these authors present clearly display C_2 at λ4737 and C_3 at λ4050 and λ3991 (although they do not comment upon this). This would suggest that the atmosphere is carbon-rich, in common with our program objects. However, CO is not detected from the source; instead it is an OH source (Likkel 1989). This suggests an oxygen-rich circumstellar envelope around a carbon-rich star. Perhaps it is an example of a star which was oxygen-rich on the AGB, leading to the present oxygen-rich shell, but which has now become carbon-rich when the outer layers were lost and carbon-rich material was mixed to the surface. A more evolved object also showing both oxygen- and carbon-rich regions is the young PN IRAS 07027−7934 (Vo–1), which has been discussed by Zijlstra et al. (1991). It possesses a carbon-rich [WC 11] central star and displays PAH features, also indicative of a carbon-rich chemistry, presumably arising from the inner edge of the circumstellar dust shell. However, it also possess an OH maser, located in the outer regions of the circumstellar shell. The authors suggest that the star has recently (last ~500 yr) transformed from oxygen-rich to carbon-rich. Several additional young PNs have been identified which show evidence for both carbon-rich (carbon-rich central star, 11.3 μm SiC feature, unidentified infrared features commonly attributed to PAHs) and oxygen-rich (18 and 9.8 μm silicate features) chemistries (Zhang & Kwok 1990). Perhaps we should note for completeness that there are several PPNs which do display a consistent oxygen-rich nature (OH maser emission, 9.7 μm silicate emission feature, and no molecular carbon in optical spectra), such as IRAS 18095+2704, 19114+0002, and 20004+2955.

Five of our six program objects have very similar *IRAS* colors, which suggests that they have similar circumstellar shell temperatures, and which may provide a guide to the identification of similar objects. All but 22223+4327 lie in a very restricted region of the *IRAS* color-color plane. Using one of the characterizations of this color-color plane, with $C_{21} = \log(12S_{25}/25S_{12})$ and $C_{32} = \log(25S_{60}/60S_{25})$, we find all five of these to lie in the range $0.20 \leq C_{21} \leq 0.45$ and $-0.90 \leq C_{32} \leq -0.65$. This region is clearly displayed in Omont et al. (1993, Fig. 8), where they have plotted a sample of *IRAS* sources with cool circumstellar shells. Their sample did not include 05113+1347, which also falls in this region. The similar colors indicate similar physical conditions, particularly similar temperatures in the circumstellar dust shells ($T \sim 200$ K), plus the effect of the 21 μm emission feature on the 25 μm band. Since all five of these objects possess the 21 μm emission feature, it may be that objects with these colors have physical conditions which represent a particularly conducive environment to the existence of the molecule producing this. Three other objects also fall in this region on their figure, 07134+1005, which we have discussed above as a carbon-rich PPN with 21 μm emission, IRAS 07430+1115, for what our recent spectra have also shown molecular C_2 (and which we will discuss elsewhere), and IRAS 18184−1623. The last of these is a bright supergiant of spectral classification B2/5 Ia(e) (Houk & Smith-Moore 1988). Based upon its inclusion in the same restricted color-color region as seven other objects, all of which are carbon-rich, one might also expect it to be carbon-rich. The *IRAS* LRS spectrum of IRAS 18184−1623 is classified as "I" (Volk & Cohen 1989), which indicates a noisy or incomplete spectrum, presumably due to the fact that the short and long bands of the LRS do not match. It shows an increase in energy from 15 to 19 μm, and a strong peak from 19 to 22 μm, similar to the 21 μm sources. However, it is lacking the 11 to 15 μm plateau seen in the 21 μm sources. The LRS spectrum of 07430+1115 shows 11 to 15 μm emission similar to the 21 μm sources, but the spectrum is relatively weak and noisy and is flat from 15 to 22 μm. Thus any 21 μm emission feature, if present, is relatively weak. It would be worthwhile to get new ground-based 20 μm spectra of each of these two objects to further investigate the presence of the 21 μm emission feature. Spectra in the 3 μm region would also be useful to see if the 3.3 and 3.4 μm features exist in these two objects. Thus the similarity in *IRAS* colors may enable us to find additional carbon-rich PPNs similar to those of this study and which also possess the 21 μm emission feature.

In summary, the presence of molecular carbon in the optical spectra of these six PPNs seems to be a distinguishing characteristic of them as a group and is shown to be correlated with several other interesting properties, in particular a 21 μm emission feature. The similarity in their *IRAS* colors may be a means to identify other similar objects. Additional studies of this group will provide further information on their properties and can lead to a better understanding of how these carbon-rich PPNs fit into the general picture of evolution from the AGB to PN phases.

I am pleased to acknowledge the assistance of the staffs of Kitt Peak National Observatory, especially D. Harmer, and Dominion Astrophysical Observatory, where these observations were made. The kind and stimulating hospitality of the DAO, where this research was conducted during a sabbatical leave, was much appreciated, as was the assistance of D. Crabtree and W. Fisher with the data reduction and D. Duncan in making the figures. This study was motivated by and profited by my continued interaction with S. Kwok in the study of PPNs. S. Kwok and D. Lambert kindly commented on a draft of this paper. The support of grants from the NASA Astrophysics Data Program (NAG 5-1223), the NASA JOVE Program (NAG 8-232), and the National Science Foundation (AST 90-18032), and the support of a University Research Professorship by Valparaiso University are also gratefully acknowledged.

REFERENCES

Barlow, M. J. 1993, in Astronomical Infrared Spectroscopy: Future Observational Directions, ed. S. Kwok (ASP Conf. Ser. 41), 97
Bond, H. E. 1991, in IAU Symp. 145, Evolution of Stars: The Photospheric Abundance Connection, ed. G. Michaud & A. Tutukov (Dordrecht: Kluwer), 341
Bujarrabal, V., Alcolea, J., & Planesas, P. 1992, A&A, 257, 701
Buss, R. H., Jr., Cohen, M., Tielens, A. G. G. M., Werner, M. W., Bregman, J. D., Witteborn, F. C., Rank, D., & Sandford, S. A. 1990, ApJ, 365, L23
Cohen, M., & Kuhi, L. V. 1977, ApJ, 213, 79
Cox, P. 1993, in Astronomical Infrared Spectroscopy: Future Observational Directions, ed. S. Kwok (ASP Conf. Ser. 41), 163
Crampton, D., Cowley, A. P., & Humphreys, R. M. 1975, ApJ, 198, L135
Geballe, T. R., Tielens, A. G. G. M., Kwok, S., & Hrivnak, B. J. 1992, ApJ, 387, L89
Geballe, T. R., & van der Veen, W. E. C. J. 1990, A&A, 235, L9
Gray, D. F. 1989, in FGK Stars and T Tauri Stars, ed. L. E. Cram & L. V. Kuhi (NASA SP-502), 7
Hinkle, K. H., Keady, J. J., & Bernath, P. F. 1988, Science, 241, 1319
Houk, N., & Smith-Moore, M. 1988, Michigan Catalog of Two-Dimensional Spectral Types for the HD Stars, 4 (Ann Arbor: Brown-Brumfield)
Hrivnak, B. J., & Kwok, S. 1991a, ApJ, 368, 564
———. 1991b, ApJ, 371, 631
Hrivnak, B. J., Kwok, S., & Geballe, T. R. 1994, ApJ, 420, 783
Hrivnak, B. J., Kwok, S., & Volk, K. M. 1989, ApJ, 346, 265
Hrivnak, B. J., Kwok, S., Volk, K. M., & Langill, P. P. 1994, in preparation
Humphreys, R. M., Warner, J. W., & Gallagher, J. S. 1976, PASP, 88, 380
Iben, I., Jr., & Renzini, A. 1983, ARA&A, 21, 271
Jaschek, C., & Jaschek, M. 1987, The Classification of Stars (Cambridge: Cambridge Univ. Press), 275
Jenkner, H., Lasker, B. M., Sturch, C. D., McLean, B. J., Shara, M. M., & Russell, J. L. 1990, AJ, 99, 2082
Keenan, P. C., & McNeil, R. C. 1976, An Atlas of Spectra of the Cooler Stars: Types G, K, M, S, and C (Columbus: Ohio State Univ. Press)
Kwok, S. 1993, ARA&A, 31, 63
Kwok, S., Hrivnak, B. J., & Geballe, T. R. 1990, ApJ, 345, L51
Kwok, S., Hrivnak, B. J., Geballe, T. R., & Langill, P. P. 1993, in Astronomical Infrared Spectroscopy: Future Observational Directions, ed. S. Kwok (ASP Conf. Ser. 41), 123
Kwok, S., Volk, K. M., & Hrivnak, B. J. 1989, ApJ, 360, L23
Lambert, D. L., Hinkle, K. H., & Luck, R. E. 1988, ApJ, 333, 917
Lattanzio, J. C. 1989, in IAU Colloq. 106, Evolution of Peculiar Red Giants, ed. H. Johnson & B. Zuckerman (Cambridge: Cambridge Univ. Press), 161
Lewis, B. M., Eder, J., & Terzian, Y. 1990, ApJ, 362, 634
Likkel, L. 1989, ApJ, 344, 350
Likkel, L., Forveille, T., Omont, A., & Morris, M. 1991, A&A, 246, 153
Luck, R. E., & Bond, H. E. 1989, ApJ, 342, 476
McKeller, A. 1948, ApJ, 108, 453
Nassau, J. J., Stephenson, C. B., & MacConnell, D. J. 1965, Luminous Stars in the Northern Milky Way Galaxy VI (Hamburg: Hamburg Sternwarte)
Ney, E. P., Merrill, K. M., Becklin, E. E., Neugebauer, G., & Wynn-Williams, C. G. 1975, ApJ, 198, L129
Olofsson, H. 1987, in Late Stages of Stellar Evolution, ed. S. Kwok & S. R. Pottasch (Dordrecht: Reidel), 149
Omont, A. 1993, in Astronomical Infrared Spectroscopy: Future Observational Directions, ed. S. Kwok (ASP Conf. Ser. 41), 87
Omont, A., Loup, C., Forveille, T., te Lintel Hekkert, P., Habing, H., & Sivaganam, P. 1993, A&A, 267, 515
Parthasarathy, M., Garcia Lario, P., & Pottasch, S. R. 1992, A&A, 264, 159
Parthasarathy, M., & Pottasch, S. R. 1986, A&A, 154, L16
Schönberner, D. 1983, ApJ, 272, 708
———. 1990, in From Miras to Planetary Nebulae: Which Path for Stellar Evolution? ed. M. O. Mennessier & A. Omont (Gif-sur-Yvette: Ed. Frontières), 355
Slijkhuis, S., Hu, J. Y., & de Jong, T. 1991, A&A, 248, 547
Swings, P., McKeller, A., & Rao, K. N. 1953, MNRAS, 113, 571
Trams, N. R., Waters, L. B. F. M., Lamers, H. J. G. L. M., Waelkens, C., Geballe, T. R., & Thé, P. S. 1991, A&AS, 87, 361
van der Veen, W. E. C. J., Habing, H. J., & Geballe, T. R. 1989, A&A, 226, 108
Volk, K., & Cohen, M. 1989, AJ, 98, 931
Volk, K. M., & Kwok, S. 1989, ApJ, 342, 345
Waelkens, C., Van Winckel, H., Bogaert, E., & Trams, N. R. 1991, A&A, 251, 495
Yamashita, Y., Nariai, K., & Norimoto, Y. 1978, An Atlas of Representative Stellar Spectra (New York: Halsted)
Zhang, C. Y., & Kwok, S. 1990, A&A, 237, 479
Zijlstra, A. A., Gaylard, M. J., te Lintel Hekkert, P., Menzies, J., Nyman, L.-Å., & Schwarz, H. E. 1991, A&A, 243, L9